Cosmic microwave background constraints for global strings and global monopoles

Article (Accepted Version)

Prepared for submission to JCAP

CMB contraints for O(2) and O(3) topological defects

Mark Hindmarsh,[a,b] **Joanes Lizarraga**[c] **Asier Lopez-Eiguren**[c] **and Jon Urrestilla**[c]

[a]Department of Physics & Astronomy, University of Sussex, Brighton, BN1 9QH, United Kingdom

[b]Department of Physics and Helsinki Institute of Physics, PL 64, FI-00014 University of Helsinki, Finland

[c]Department of Theoretical Physics, University of the Basque Country UPV/EHU, 48080 Bilbao, Spain

E-mail: m.b.hindmarsh@sussex.ac.uk, joanes.lizarraga@ehu.eus, asier.lopez@ehu.eus, jon.urrestilla@ehu.eus

Abstract. We present cosmic microwave background (CMB) power spectra from recent numerical simulations of topological defects in the $O(N)$ model, with $N = 2, 3$, and compare them to CMB power spectra measured by *Planck*. We obtain constraints ...

Contents

1 Introduction

Mention $O(N)$, and that in the paper with Dani there was a difference between $N < 4$ and $N > 4$, where the latter was better approximated by large N results? Also, $N = 2$ and $N = 3$ have extended objects, so not only because N is low is the approximation worse.

2 Model and Method overview

The simplest field theory model that contains global topological defects is the global $O(N)$ theory, where $O(N)$ global symmetry spontaneously breaks down to $O(N-1)$. The action that gives rise to this kind of defects is [1],[],

$$\mathcal{S} = \int d^4x\sqrt{-g}\Big(\frac{1}{2}\partial_\mu\Phi^i\partial^\mu\Phi^i - \frac{1}{4}\lambda(|\Phi|^2-\eta^2)^2\Big), \tag{2.1}$$

where Φ^i, $i = 1, .., N$ are real fields, $|\Phi| \equiv \sqrt{\Phi^i\Phi^i}$ and λ and η are real constant parameters. In the symmetry breaking a massive particle with mass $m_s = \sqrt{2\lambda}\eta$ arises as well as massless Goldstone bosons. The number of Goldstone bosons depends on the value of N, for example, for $N = 2$ just one boson appears while for $N = 3$ two bosons are present. The energy of local defects is divergent with radius but in a cosmological situation this divergence is not catastrophic, since other defects around cut-off the energy divergence. Moreover, the presence of the Goldstone bosons allows the defects to lose energy by their production. All this leads to dynamics that are different from the dynamics of local defects. For example, global monopoles reach a scaling regime, whereas local monopoles could be catastrophic for the viability of a universe that produced them at high enough energies.

Since our aim is to study the dynamics of a network of global defects in a expanding universe, we consider a flat Friedmann-Robertson-Walker space-time with comoving coordinates:

$$ds^2 = a^2(\tau)(d\tau^2 - dx^2 - dy^2 - dz^2), \tag{2.2}$$

where $a(\tau)$ is the cosmic scale factor and τ is conformal time. The equations of motion derived from (2.1) are

$$\ddot{\phi}^i + 2\frac{\dot{a}}{a}\dot{\phi}^i - \nabla^2\phi^i = -a^2\lambda(\phi^2 - \eta^2)\phi^i, \tag{2.3}$$

and the dots represent derivatives with respect to the conformal time τ.

Since the size of the defect is given by their mass ($\delta \sim m_s^{-1}$), it is a fixed length in physical units, which means that in comoving coordinates the size of the defects rapidly decreases. Thus, in order to account for this effect, one has either to choose the parameters of the model with extreme care or or one has to use the Press-Ryden-Spergel algorithm [], which is widely used in numerical simulations of defects []. The validity of the algorithm has been proved in several works, where the errors due to the algorithm are shown to be typically smaller than the statistical errors, or the systematic errors inherent to the discretization procedure. This algorithm makes the width of the defect controllable by turning the coupling constant into a time-dependent variable:

$$\lambda = \lambda_0 a^{-2(1-s)}, \tag{2.4}$$

where the parameter s is the responsible to control the defect size. That is, when the $s = 0$ the defect size is fixed in comoving coordinates and when $s = 1$ we obtain the true case where the size of the defect is fixed in physical length.

The evolution of a defect network perturbs the background space-time; and those perturbations evolve and affect the contents of the universe, eventually creating CMB anisotropies. In contrast to the inflationary perturbations, which were seeded primordially and then evolve "passively", defects induce perturbations actively during their whole existence. Those for Abelian Higgs cosmic strings are estimated to be roughly of the order of the magnitude of $G\mu$, where G is Newton's constant and μ the string tension. Current bounds on $G\mu$ constrain its value to be below 10^{-6} [2–5].

Energy-momentum correlations are an effective statistical tool used to describe defect induced perturbations. Indeed, the unequal time correlators of the energy-momentum tensor are the only objects needed to derive the power spectrum of CMB anisotropies. UETCs are defined as follows:

$$U_{\lambda\kappa\mu\nu}(\mathbf{k}, \tau, \tau') = \langle \mathcal{T}_{\lambda\kappa}(\mathbf{k}, \tau)\mathbf{T}_{\mu\nu}(\mathbf{k}, \tau')\rangle, \tag{2.5}$$

where $\mathbf{T}_{\alpha\beta}(\mathbf{k}, \tau)$ is the energy momentum tensor.

In principle considering all possible degrees of freedom of the energy-momentum tensor, there seem to be $\frac{1}{2}10(10+1) = 55$ such correlators that would be functions of 5 variables (3 components of $\mathbf{k}$ plus two times). Fortunately, rotational symmetry simplifies the problem considerably. On the one hand the correlators only depend on 3 variables: k (the magnitude of $\mathbf{k}$), τ and τ'.

On the other hand, the UETCs can be projected out into scalar, vector and tensor parts; but the two vector and the two tensor components are related by parity for a symmetric source (which is the case). Hence, we can write

$$U_{ab}(\mathbf{k}, \tau, \tau') = \frac{\eta^4}{\sqrt{\tau\tau'}}\frac{1}{V}C_{ab}(k, \tau, \tau'), \tag{2.6}$$

where η is the symmetry breaking scale, V a formal comoving volume factor, and the functions $C_{ab}(k, \tau\tau')$ defined by this equation are dimensionless. The indices a, b take four values corresponding to the independent components of the energy momentum tensor: two scalar,

one vector and one tensor. We will denote the scalar indices 1 and 2 (corresponding to the longitudinal gauge potentials ϕ and ψ), the vector component with 'v' and the tensor component with 't'. Note that the scalar, vector and tensor contributions are decoupled for linearized cosmological perturbations, and therefore cross correlators between them vanish, except in the scalar sector: hence the UETC group os reduced to just 5 independent correlators.

The UETCs give the power spectra of cosmological perturbations when convolved with the appropiate Green's functions. In practice, they are decomposed into a set of functions derived from the eigenvectors of the UETCs, which are used as sources for an Einstein-Boltzmann integrator. The power spectrum of interest is reconstructed as the sum of power spectra from each of the source functions.

A further simplification occurs when the times τ and τ' are both in epochs during which the scale factor grows with the same constant power of conformal time. In this case the correlation functions do not depend on k, τ and τ' separately, but only on $k\tau$ and $k\tau'$. This behaviour is called scaling, and scaling correlators can be written

$$U_{ab}(\mathbf{k}, \tau, \tau') = \frac{\eta^4}{\sqrt{\tau\tau'}} \frac{1}{V} \bar{C}_{ab}(k\sqrt{\tau\tau'}, \tau'/\tau). \tag{2.7}$$

Here, the overbar represents the scaling form of the UETC in a FLRW background. We will sometimes write $z = k\sqrt{\tau\tau'}$, $r = \tau'/\tau$. An alternative pair of scaling variables is $x, x' = k\tau, k\tau'$. A scaling UETC will have eigenvectors which depend on k and τ only through the combination x.

Scaling in an immensely valuable property, as it allows to extrapolate numerical simulations to the required cosmological scales. However, perfect scaling is not a feature of the true UETCs, as the universe undergoes a transition from radiation-dominated to matter-dominated expansion during times of interest[1]. Hence the UETCs will also depend explicitly on τ_{eq}, the time of equal radiation and matter density.

3 UETCs from the Simulations

In this section we present the details of the numerical simulations from which the UETC data was collected, and how the data was merged into a set of 5 scaling UETCs in each cosmological era (radiation and matter). These merged scaling UETCs are the inputs for the next section, in which the eigenvector decomposition method is described.

3.1 Simulation details

In order to simulate the evolution of the global defects in a discrete box we discretise the action (2.1) instead of solving directly the equations of motion. Then, the equations of motion are obatined from the discretized action and they are translated into a cartesian grid using standard techniques []; lattice link variable and leapfrog technique. Finally the equations are evolved in 1024^3 lattices with periodic boundary conditions where the simulations are paralellized using the LatField2 library for parallel field theory simulations []. At this point it is necessary to comment that the periodic boundary conditions impose an upper limit on the time that the system can be evolved before it feels the effects of the conditions. The simulation can only be believed up to half light-crossing time, that is, if we sent a light ray

[1] In this work we will not consider the transtion from matter-domination to Λ-domination, since its effect is rather small, as shown in [6]

	$O(2)$	$O(3)$
τ_{ini}	50	0
τ_{diff}	70	20
τ_{ref}	150	60
τ_{end}	300	250
n_{out}	50	60

Table 1. Maybe the table could be called later, when we know what the different parameters mean?

τ_{eq}	300	150	40	10	3
τ_{ref}/τ_{eq}	0.5	1.0	3.75	15	50
τ_{end}/τ_{eq}	1.00	2.0	7.5	50	100
$\alpha(\tau_{ref})$	1.09	1.17	1.44	1.76	1.91
$\alpha(\tau_{end})$	1.17	1.29	1.60	1.86	1.95

Table 2. Similarly, maybe called later?

in opposite directions in the box, the simulation is accurate up to when the two rays meet again.

Our simulation lattice has a comoving spatial separation of $dx = 0.5$ and time steps of $dt = 0.1$, in units where $\eta = 1$. The simulation volume therefore has comoving size $L = 512$. The coupling was chosen to be $\lambda = 2$, and thus the mass of the scalar fields $m = \sqrt{2}e\eta$. These simulations were performed in Sisu, a Massively Parallel Processor (MPP) supercomuter managed by CSC-IT center for science. We performed 5 individual runs in pure radiation and in pure matter dominated eras to determine the scaling form of the UETCs. We also performed runs across the radiation-matter cosmological transitions using the same configuration, the information of those runs can be seen in Table 2 **maybe call the table later, we do not know what all those parameters mean**.

In the initial field configuration, the scalar field velocities are set to zero and the scalar fields are set to be stationary Gaussian random fields with power spectrum

$$P_\phi(\mathbf{k}) = \frac{A}{1 + (kL_\phi)^2}, \tag{3.1}$$

with A chosen so that $\langle|\phi^2|\rangle = \eta^2$, and $L_\phi = 5\eta^{-1}$.

The UETCs cannot be calculated until after the defects are formed and reach their scaling configuration. These early phases contain a huge amount of excess energy induced by the random initial conditions, therefore we smooth the field distribution by applying a period of diffusive evolution, with the second derivatives removed from the equations of motion. Depending on the model we are simulating we have to impose the diffusive evolution in a different time period. The parameters and details of each case can be found in Table 1.

We measure the UETC by recording the mean value of $C_{ab}(k, \tau_{ref}, \tau)$ for wavevectors binned in the range $2\pi(n-1)/L < |\mathbf{k}| \leq 2n/L$ $(1 \leq n < N_b)$, with $N_b =$ **how much is this, Asier?**, and n_{out} logarithmically-spaced times between τ_{ref} and τ_{end}. The wavenumber of the nth bin k_n is set to the mean value of $|\mathbf{k}|$ in that bin. Table 1 shows the values of the parameters.

We also record the equal time correlators (ETCs) at each time the UETC is evaluated, with which we can monitor the quality of scaling. Perfect scaling would mean that the ETCs collapse to a single line when plotted against $x = k\tau$.

3.2 Scaling

In order to compare simulations with different initial conditions is better to define the *physical* time based on the state of the defect network itself, and in particular to use a length scale in the network. We will define two different length scales, one for each case of defect under study; i.e., one for strings and one for monopoles.

For the case of strings the comoving string separation ξ_s has been identified as a useful quantity to determine compatible simulation stages. The string separation is defined in terms of the mean string length L_s in a horizon volume V as

$$\xi = \sqrt{\frac{V}{L_s}}. \tag{3.2}$$

The mean string length, L_s, is usually derived by directly measuring the comoving length of each string (see details in []). One way of obtaining the length of strings is by summing the number of plaquettes pierced by strings. Such plaquettes are identified working out the winding of the field in each plaquette of the lattice. An alternative way is to use local field theory estimators to get the above ratio []. In our case we use the mean Lagrangian density $\bar{\mathcal{L}}$, with

$$L_s = -\bar{\mathcal{L}}V/\mu, \tag{3.3}$$

where μ is the energy per unit length of the string.

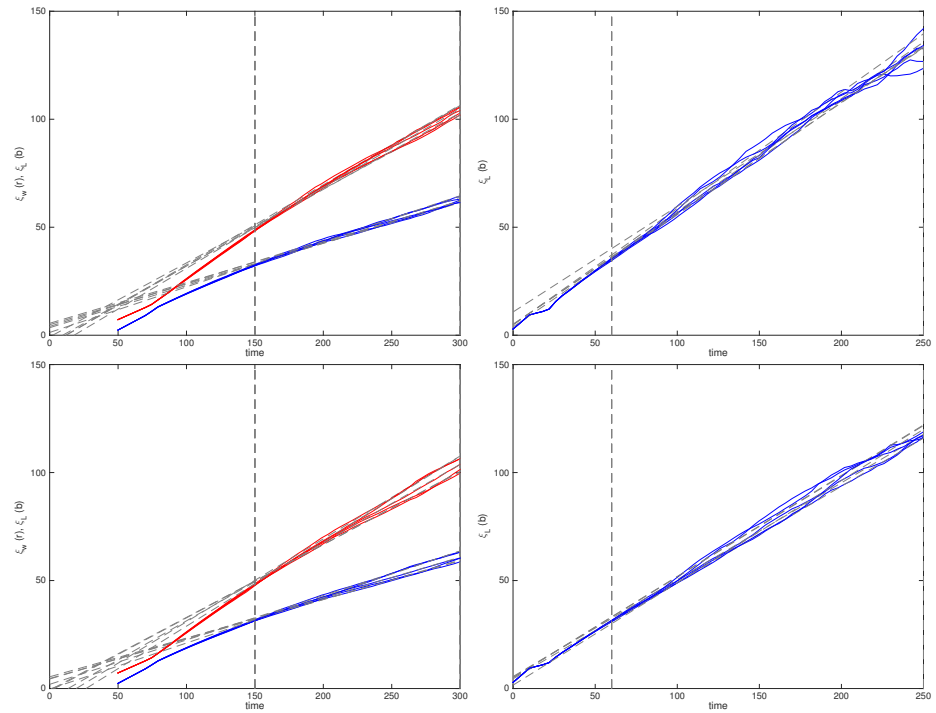

Numbers and labels bigger! There is no ξ_{L_s} or ξ_{L_M} in the figure. What is ξ_W? Not defined in text!

Figure 1. example caption

Monopole networks can be characterized using the comoving monopole separation ξ_m. The monopole separation is defined in terms of the monopole number in a horizon volume V

	ξ_W	ξ_{L_s}	ξ_{L_M}
Radition	0.36 ± 0.01	0.20 ± 0.01	0.52 ± 0.02
Matter	0.36 ± 0.02	0.19 ± 0.01	0.46 ± 0.01

Table 3.

as

$$\xi_m = \left(\frac{V}{\mathcal{N}}\right)^{1/3} \tag{3.4}$$

where $\mathcal{N}$ is the monopole number in the volume V[2]. The monopole number can be computed by directly obtaining the topological charge in each lattice cell of the simulation box [].

Using local field theory estimators, $\mathcal{N}$ can be obtained using the mean Lagrangian density $\bar{\mathcal{L}}$

$$\mathcal{N} = -\bar{\mathcal{L}}V/\mu_m, \tag{3.5}$$

where μ_m is a energy of a monopole.

As we can see in Fig. 1 the scaling information given by both approaches (i.e., length estimations counting windings or the monopole topological charge, or using field estimators) are compatible. The computational cost of the field estimators in considerably lower, therefore we will use just the local field theory estimators to analyse the scaling regime.

As was found in previous works, the asymptotic behaviour of the separations for both type of defects is very close to linear,

$$\xi \to \beta(\tau_{sim} - \tau_{offset}), \tag{3.6}$$

where τ_{offset} is the time offset of the ξ curve (see Fig. 1). We have managed to choose initials conditions such that the time offset is almost zero in all the realisations. Although the ξ are almost equal we will define the mean slope β as the average of all different slopes from different realizations. Numerical values of the slopes can be found in Table 3.

Since the offset is zero in our simulations, we can directly merge the UETCs obtained from different realizations. We performed simulations, for both strings and monopoles, 5 times in Radiation domination and 5 times in Matter dominations. Figure 2 shows the averaged Matter UETC for global strings, and Fig. 3 shows the corresponding one for global monopoles.

4 UETC interpolation functions and diagonalisation

Once that it has been established that the simulations reach scaling, the (scaling) UETCs have been output and averaged, we need to use that information to estimate the true (non-scaling) UETCs $C_{ab}(k, \tau, \tau')$. There are several proposals in the literature for performing this estimation. However, we will follow the *Fixed-k interpolation* proposed in []: the UETCs are thought of as symmetric functions of τ and τ' for a given k. This approach also fits very well into the scheme used by Einstein-Boltzmann codes, which solve the perturbation equations with an outer loop over k and an inner time integration for fixed values of k.

This method constructs approximations to $C_{ab}(k, \tau, \tau')$ from the scaling matter and radiation sources, at each value of k. The relative mixture of matter and radiation UETCs

[2]We will not make any distinction between monopoles and antimonopoles in this work, since for our purposes they are equivalent. Therefore, we will denote as $\mathcal{N}$ the sum of monopoles and antimonopoles

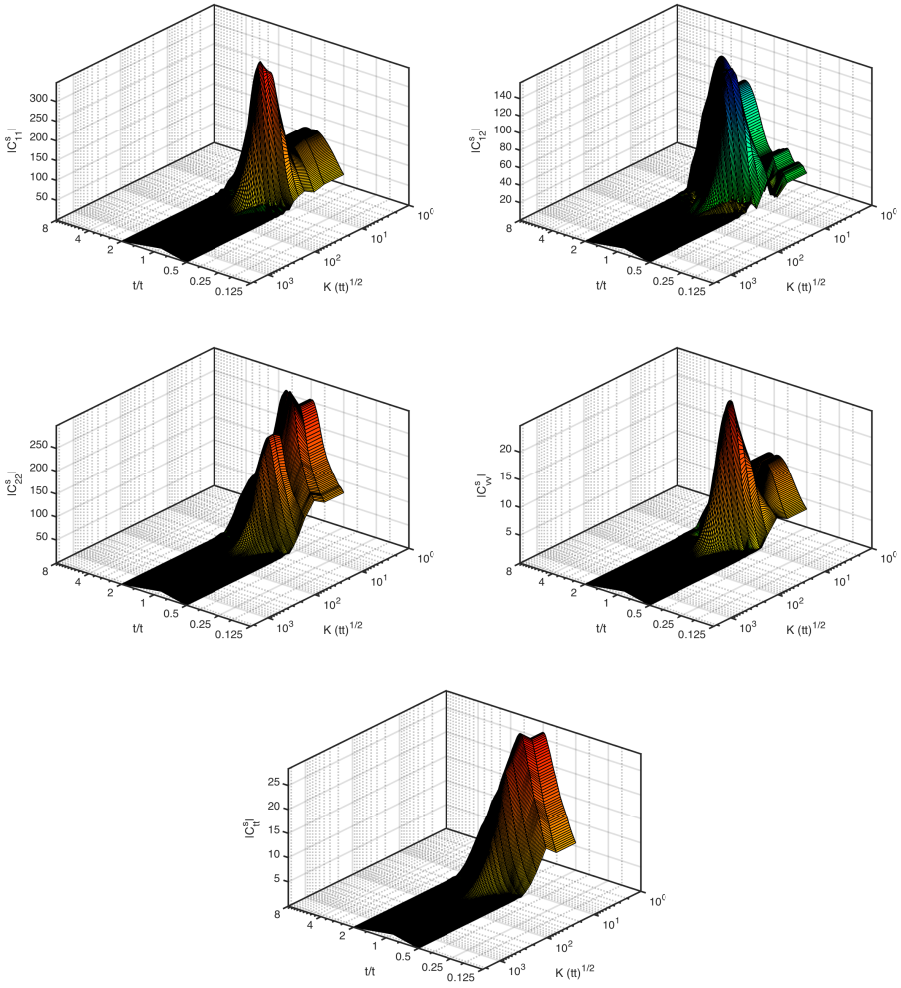

Figure 2. UETCs for Matter era O(2)

is determined by τ/τ_{eq} and τ'/τ_{eq}. A proposal for the UETCs which models this behaviour across the radiation-matter transition is

$$C_{ab}(k,\tau,\tau') = f\Big(\frac{\sqrt{\tau\tau'}}{\tau_{eq}}\Big)\bar{C}^M_{ab}(k\tau,k\tau') + \Big(1 - f\Big(\frac{\sqrt{\tau\tau'}}{\tau_{eq}}\Big)\Big)\bar{C}^R_{ab}(k\tau,k\tau'). \tag{4.1}$$

This is manifestly symmetric in τ,τ'. It approximates the UETC in the entire region $\tau\tau' \sim \tau^2_{eq}$ by the linear combination of pure radiation and pure matter era scaling correlators at extreme values of τ/τ_{eq}. At sufficiently unequal times bracketing τ_{eq} the true UETC may depart significantly from the model, but this should not matter in practice as the UETC is very small there for any value of k.

We note that the source functions for the EB integrators at a given k are now just the eigenvectors of these model UETCs, multiplied by the square root of the associated eigenvalues, and so they are indeed orthogonal.

The interpolating function f is not a known function. There was a proposal by the authors of [**?**] where they calculate the function f for large N $O(N)$ models, and then they comment on the possibility of that function being universal. However, in [] it was shown that

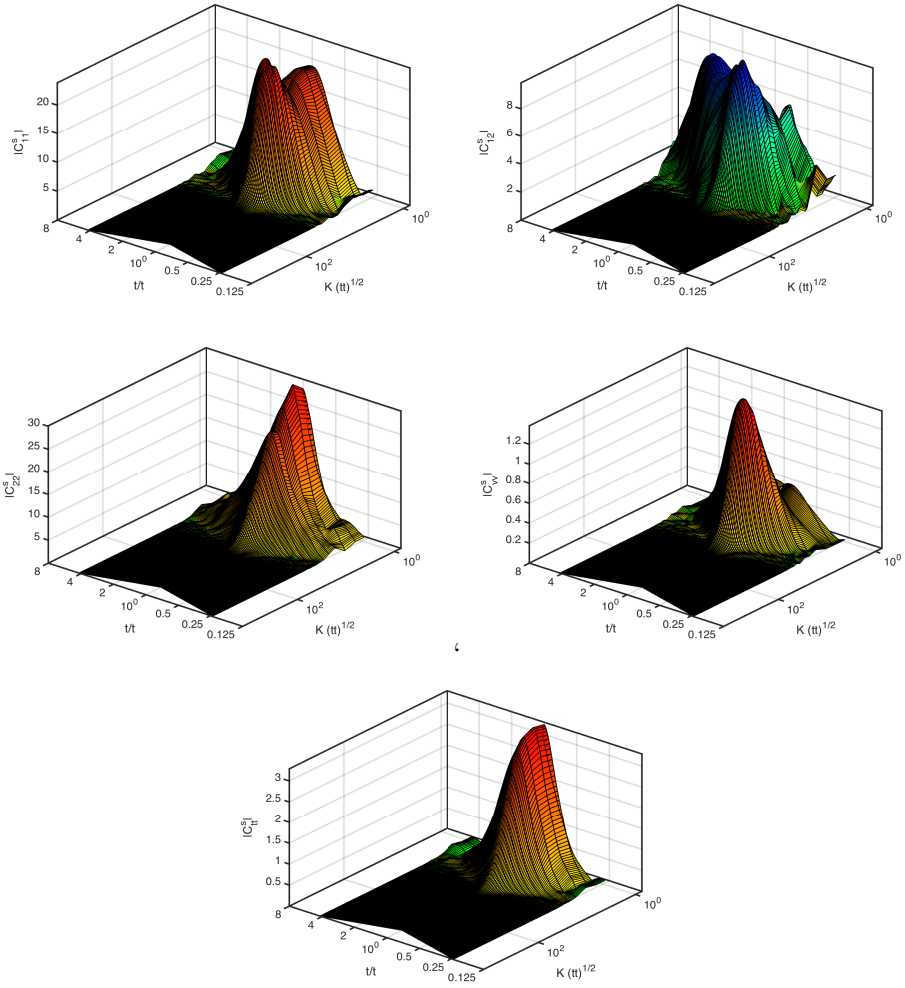

Figure 3. UETCs for Matter era O(3)

for the Abelian Higgs strings the interpolating function was different. Therefore, we need to calculate what the interpolating function is for these two specific defects.

We adopt the recipe given in [] to define the function such that it should reproduce the equal-time correlators $E_{ab}(k,\tau) = C_{ab}(k,\tau,\tau)$. First we define

$$f_{ab}(k,\tau) = \frac{E^{RM}_{ab}(k,\tau) - \bar{E}^{M}_{ab}(k\tau)}{\bar{E}^{R}_{ab}(k\tau) - \bar{E}^{M}_{ab}(k\tau)} \quad \forall k, \tag{4.2}$$

where $\bar{E}^{R}(k\tau)$ and $\bar{E}^{M}(k\tau)$ are the scaling ETCs in the radiation and matter eras respectively, and $E^{RM}(k,\tau)$ is the true ETC during the transition.

We will see that the functions $f_{ab}(k,\tau)$ extracted from our simulations are consistent with being independent of k and thus the above definition will reproduce Eq **??** when evaluated in equal times. We will also see that it is a good approximation to take the same function $f(\tau)$ for each of the five ETCs.

We extracted ETCs from the simulations with τ_{eq} = 3,10,40,150 and 300, and used Eq. (4.2) to compute the function $f(\tau)$. Fig. 4 shows the results obtained for correlators scalar11

	ζ	η
O(2)	0.26 ± 0.03	1.15 ± 0.02
O(3)	0.23 ± 0.05	1.4 ± 0.2

Table 4.

and vector for global strings, the transition functions for the rest of the correlators and for the global monopole case are similar to those shown in the figure. The five grey shaded regions represent the raw transition functions obtained during the five transition periods simulated. The two grey levels indicate 1σ and 2σ deviations from the mean value calculated averaging over a set of wavevectors much less than the inverse string width: ?? $< |\mathbf{k}| <$??. We also include in the pictures the best-fit (solid red line) obtained fitting data using the following functional form:

$$f(\tau) = \left(1 + \zeta \frac{\tau}{\tau_{eq}}\right)^{\eta}. \tag{4.3}$$

The narrowness of the shaded regions confirms the initial assuption of the scale independence of the function.

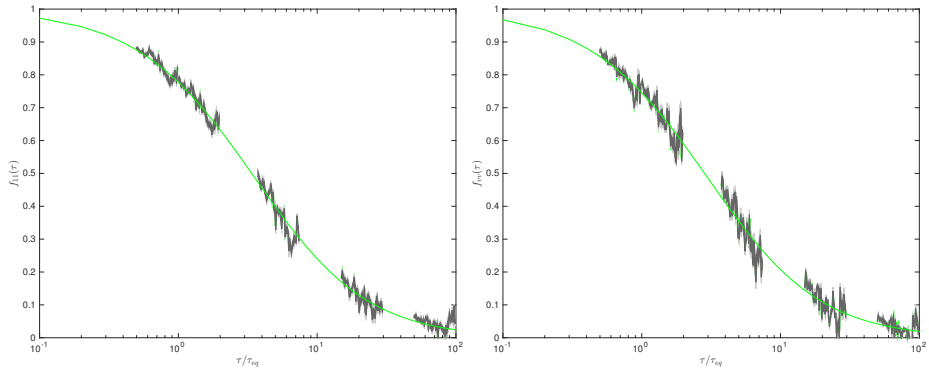

Figure 4. example caption

Table 4 shows the mean values and standard deviations for the parameters of Eq. 4.3.

5 Power Spectra

In the previous section we have defined the source functions for the global strings and monopoles. Inserting these functions into a source enabled Einstein-Boltzmann (EB) solver we can compute the contributions to CMB power spectra due to the presence of global defects. In our case the EB solver we have used is the source enabled version of CMBEASY []. The code has been additionally modified to handle source functions of that we have explained in the previous section.

The cosmological parameters used for these calculations are the best-fit values obtained by the Planck collaboration []: $h = 0.6726$, $\Omega_b h^2 = 0.02225$, $\Omega_\Lambda = 0.6844$ and reionization optical depth $\tau_{re} = 0.079$. After diagonalisation, the total contribution of defects under analysis to temperature and polarization anisotropies is calculated summing the contribution of each individual source functions.

Fig. 5 shows the temperature and all polarization channels for the CMB power spectra obtained for the global string case. Fig. 6 shows the same but for the global monopole case.

$O(3)$ is in general more oscilatory, as it should (?), for TT, EE. But why not in BB ?

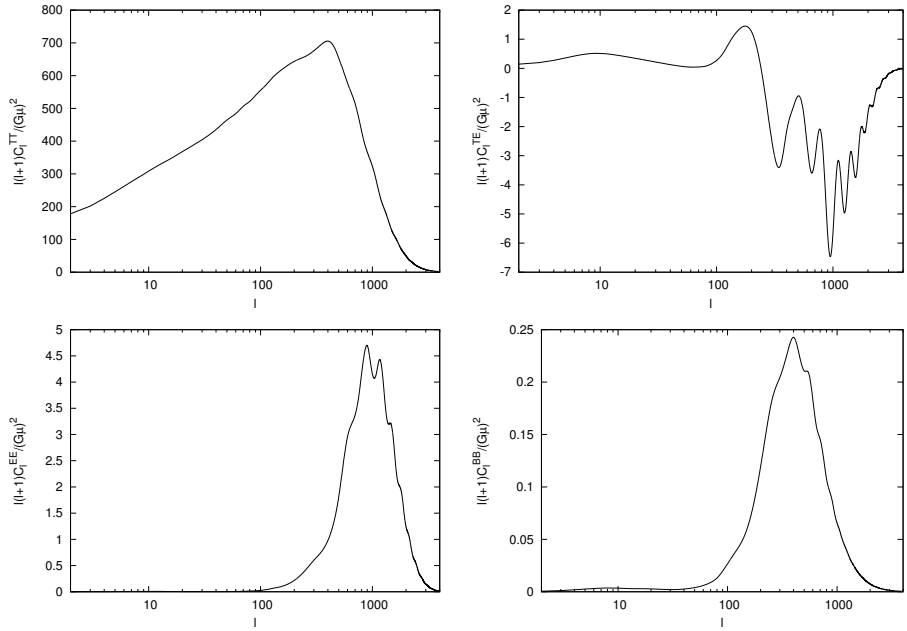

Figure 5. example caption

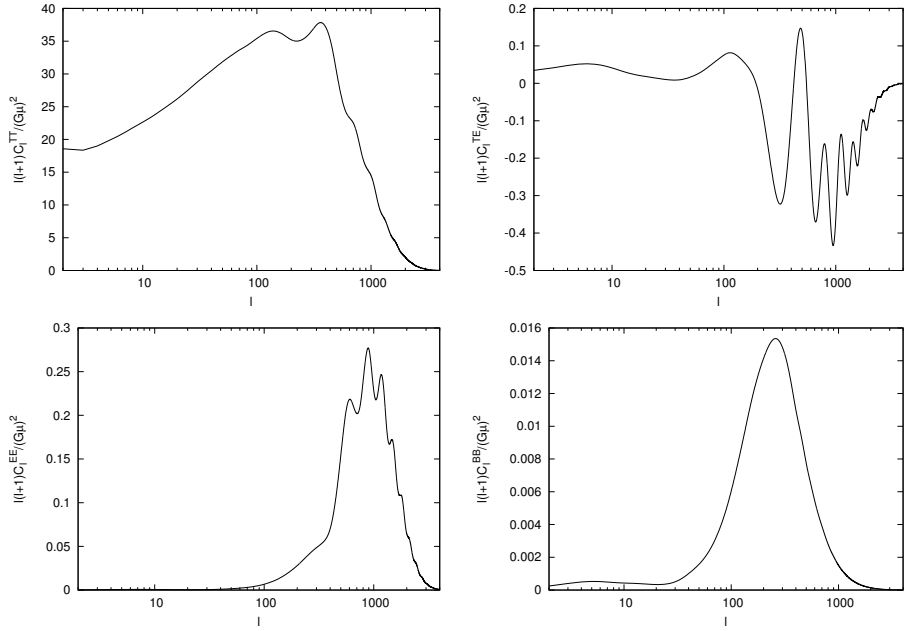

Figure 6. example caption

6 Fits and constraints

We use *Planck* 2015 CMB temperature and polarization likelihoods and data [7, 8] to put limits on the allowed fraction of global strings and monopoles and on other cosmological parameters. In some cases we also include into the analysis the prior set by the Hubble Space Telescope (HST) [9] on the parameter H_0. We always vary the standard six ΛCDM parameters of the basic inflationary model or "power-law" ($\mathcal{PL}$) model, $\omega_b, \omega_c, \Theta_{MC}, \tau, \ln 10^10 A_s, n_s$ and

Dataset	*Planck* 2015 CMB		*Planck* 2015 CMB + HST	
Model	$\mathcal{PL}+G\mu$	$\mathcal{PL}$	$\mathcal{PL}+G\mu$	$\mathcal{PL}$
f_{10}	< 0.015	–	< 0.016	–
$10^{12}(G\mu)^2$	< 0.034	–	< 0.033	–
$-\ln\mathcal{L}_{\max}$	6472	6472	6477	???

Table 5. 95% upper limits for $(G\mu)^2$ and f_{10} as well as best-fit likelihood values for different cosmological models for $O(2)$ global strings, fitting for the *Planck* 2015 TT, TE, EE and low TEB data alone and in combination with the prior set by HST in the value of H_0.

Dataset	*Planck* 2015 CMB		*Planck* 2015 CMB + HST	
Model	$\mathcal{PL}+G\mu$	$\mathcal{PL}$	$\mathcal{PL}+G\mu$	$\mathcal{PL}$
f_{10}	< 0.024	–	< 0.026	–
$10^{12}(G\mu)^2$	< 0.73	–	< 0.79	–
$-\ln\mathcal{L}_{\max}$	6470	6472	6476	???

Table 6. 95% upper limits for $(G\mu)^2$ and f_{10} as well as best-fit likelihood values for different cosmological models for $O(3)$ defects, fitting for the *Planck* 2015 TT, TE, EE and low TEB data alone and in combination with the prior set by HST in the value of H_0.

the nuisance parameters inherent to the experiment (not shown here).

Tables **??** and **??** show the results for strings and monopoles respectively. define f10 somewhere. And maybe $G\mu$ for monopoles also!

- O(2) does not improve the fit
- O(3) improves slightly the fit, 6472->6470, however one more parameter, is not significant.
- Baseline with planck + hst still running

7 Discussion and conclusions

We have calculated the CMB power spectra from the energy-momentum correlations computed in numerical simulations of a networks of global strings and monopoles. Then we compared the CMB power spectra obtained to Planck CMB power spectra.

References

[1] M. Barriola and A. Vilenkin, *Gravitational Field of a Global Monopole*, *Phys. Rev. Lett.* **63** (1989) 341.

[2] **Planck Collaboration** Collaboration, P. Ade *et. al.*, *Planck 2013 results. XXV. Searches for cosmic strings and other topological defects*, *Astron.Astrophys.* **571** (2014) A25, [arXiv:1303.5085].

[3] J. Urrestilla, N. Bevis, M. Hindmarsh, and M. Kunz, *Cosmic string parameter constraints and model analysis using small scale Cosmic Microwave Background data*, *JCAP* **1112** (2011) 021, [arXiv:1108.2730].

[4] J. Lizarraga, J. Urrestilla, D. Daverio, M. Hindmarsh, M. Kunz, and A. R. Liddle, *Constraining topological defects with temperature and polarization anisotropies*, *Phys. Rev.* **D90** (2014), no. 10 103504, [arXiv:1408.4126].

[5] A. Lazanu, E. P. S. Shellard, and M. Landriau, *CMB power spectrum of Nambu-Goto cosmic strings*, *Phys. Rev.* **D91** (2015), no. 8 083519, [arXiv:1410.4860].

[6] J. Lizarraga, J. Urrestilla, D. Daverio, M. Hindmarsh, and M. Kunz, *New CMB constraints for Abelian Higgs cosmic strings*, *JCAP* **1610** (2016), no. 10 042, [arXiv:1609.0338].

[7] **Planck** Collaboration, N. Aghanim *et. al.*, *Planck 2015 results. XI. CMB power spectra, likelihoods, and robustness of parameters*, *Submitted to: Astron. Astrophys.* (2015) [arXiv:1507.0270].

[8] **Planck** Collaboration, P. A. R. Ade *et. al.*, *Planck 2015 results. XIII. Cosmological parameters*, arXiv:1502.0158.

[9] A. G. Riess *et. al.*, *A 2.4% Determination of the Local Value of the Hubble Constant*, *Astrophys. J.* **826** (2016), no. 1 56, [arXiv:1604.0142].